Brain, Behavior, and Immunity 118 (2024) 437–448

Contents lists available at ScienceDirect

Brain Behavior and Immunity

journal homepage: www.elsevier.com/locate/ybrbi

Knockdown of *Tlr3* in dorsal striatum reduces ethanol consumption and acute functional tolerance in male mice

Geoffrey A. Dilly [a,b,c,d], Yuri A. Blednov [a], Anna S. Warden [a], Lubov Ezerskiy [a,c], Caleb Fleischer [a,c], Jesse D. Plotkin [a,c], Shruti Patil [a], Elizabeth A. Osterndorff-Kahanek [a], Jody Mayfield [a], R. Dayne Mayfield [a,c], Gregg E. Homanics [e], Robert O. Messing [a,b,c,d,*]

[a] *Waggoner Center for Alcohol and Addiction Research, The University of Texas at Austin, Austin, TX 78712, United States*
[b] *Institute for Neuroscience, The University of Texas at Austin, Austin, TX 78712, United States*
[c] *Department of Neuroscience, The University of Texas at Austin, Austin, TX 78712, United States*
[d] *Department of Neurology, Dell Medical School, The University of Texas at Austin, Austin, TX 78712, United States*
[e] *Departments of Anesthesiology & Perioperative Medicine, Neurobiology, and Pharmacology & Chemical Biology, University of Pittsburgh, Pittsburgh, PA 15261, United States*

ARTICLE INFO

Keywords:
Tlr3$^{F/F}$ mice
Tlr3 knockdown in dorsal striatum
Two-bottle choice every-other-day ethanol consumption
Rotarod ataxia
Acute functional tolerance to ethanol
Diazepam
Poly(I:C)

ABSTRACT

Systemic activation of toll-like receptor 3 (TLR3) signaling using poly(I:C), a TLR3 agonist, drives ethanol consumption in several rodent models, while global knockout of *Tlr3* reduces drinking in C57BL/6J male mice. To determine if brain TLR3 pathways are involved in drinking behavior, we used CRISPR/Cas9 genome editing to generate a *Tlr3* floxed (*Tlr3*$^{F/F}$) mouse line. After sequence confirmation and functional validation of *Tlr3* brain transcripts, we injected *Tlr3*$^{F/F}$ male mice with an adeno-associated virus expressing Cre recombinase (AAV5-CMV-Cre-GFP) to knockdown *Tlr3* in the medial prefrontal cortex, nucleus accumbens, or dorsal striatum (DS). Only *Tlr3* knockdown in the DS decreased two-bottle choice, every-other-day (2BC-EOD) ethanol consumption. DS-specific deletion of *Tlr3* also increased intoxication and prevented acute functional tolerance to ethanol. In contrast, poly(I:C)-induced activation of TLR3 signaling decreased intoxication in male C57BL/6J mice, consistent with its ability to increase 2BC-EOD ethanol consumption in these mice. We also found that TLR3 was highly colocalized with DS neurons. AAV5-Cre transfection occurred predominantly in neurons, but there was minimal transfection in astrocytes and microglia. Collectively, our previous and current studies show that activating or inhibiting TLR3 signaling produces opposite effects on acute responses to ethanol and on ethanol consumption. While previous studies, however, used global knockout or systemic TLR3 activation (which alter peripheral and brain innate immune responses), the current results provide new evidence that brain TLR3 signaling regulates ethanol drinking. We propose that activation of TLR3 signaling in DS neurons increases ethanol consumption and that a striatal TLR3 pathway is a potential target to reduce excessive drinking.

1. Introduction

Some effects of chronic ethanol in the brain are mediated through toll-like receptors (TLRs) and their innate immune signaling components (Erickson et al., 2019; Meredith et al., 2021; Ramos et al., 2022; Vetreno et al., 2021). We have been interested in TLR3 since we and others have shown that TLR3 signaling plays a role in voluntary ethanol consumption in different rodent models (Blednov et al., 2021; Gano et al., 2022; Lovelock et al., 2022; Randall et al., 2019; Warden et al., 2019a). Unlike TLR4, which signals through both the MyD88 (myeloid differentiation primary response 88) and the TRIF (TIR-domain-containing adaptor inducing interferon-β) pathways, TLR3 is thought to signal only through TRIF (Kawasaki and Kawai, 2014). TLR3 responds to pathogen-associated and endogenous danger-associated molecular patterns, such as viral-derived double-stranded RNAs (Lester and Li, 2014). TLR3 activation promotes production of proinflammatory cytokines and type 1 interferons (Kawasaki and Kawai, 2014). Chronic ethanol exposure also induces proinflammatory genes and has been shown to increase expression of *Tlr3* mRNA and protein and to potentiate induction of cytokines by polyinosinic:polycytidylic acid [poly(I:C)] in mouse brain

* Corresponding author at: The University of Texas at Austin, 1601-B Trinity Street, HDB 5.320, Mail Stop Z0700, Austin, TX 78712, United States.
E-mail address: romessing@austin.utexas.edu (R.O. Messing).

https://doi.org/10.1016/j.bbi.2024.03.021
Received 16 August 2023; Received in revised form 5 March 2024; Accepted 15 March 2024
Available online 16 March 2024

(Qin and Crews, 2012). In addition, chronic ethanol drinking increases *Tlr3* mRNA and components of the TRIF-dependent pathway in mouse prefrontal cortex (PFC) and nucleus accumbens (McCarthy et al., 2018).

Several studies have shown that the TLR3 agonist poly(I:C) increases ethanol consumption in different rodent models. For example, repeated activation of TLR3 by poly(I:C) increased two-bottle choice, every-other-day (2BC-EOD) ethanol drinking in C57BL/6J male mice (Warden et al., 2019a) and increased ethanol intake in Long-Evans male rats previously trained to self-administer ethanol (Randall et al., 2019). Repeated administration of poly(I:C) also increased operant self-administration of ethanol in female and male Long-Evans rats (Lovelock et al., 2022). In addition, persistent escalation of drinking was observed in ethanol-dependent C57BL/6J male mice after poly(I:C) challenge (Gano et al., 2022). We have shown that poly(I:C) reaches the brain after systemic administration in C57BL/6J mice, and repeated administration during chronic ethanol drinking increases expression of TRIF-dependent immune transcripts in the PFC from male mice (Warden et al., 2019a).

In contrast to the ability of systemic TLR3 activation to increase voluntary ethanol consumption, global TLR3 deletion significantly reduced 2BC-EOD drinking in male but not female C57BL/6J mice (Blednov et al., 2021). Compared with their wild-type littermates, *Tlr3* knockout male mice were more sensitive to the intoxicating effects of ethanol and diazepam, suggesting regulation of GABAergic signaling by TLR3. Also, the decreased ethanol consumption was associated with decreased acute functional (behavioral) tolerance to ethanol (Blednov et al., 2021). These effects on 2BC-EOD drinking and acute functional tolerance (AFT) were opposite to those produced by deletion of MyD88 in male mice (Blednov et al., 2017; Blednov et al., 2021).

While there is considerable evidence that manipulation of TLR3 regulates ethanol consumption in rodent models, this work is based on global genetic knockout or systemic poly(I:C) treatment, which can have marked peripheral immune effects. Thus, in the current study, we tested the ability of TLR3 signaling specifically in the brain to regulate ethanol drinking and behaviors that influence drinking. TLR3 is broadly expressed in the brain among different cell types, so we generated a *Tlr3*$^{F/F}$ mouse line to selectively knockdown *Tlr3* in different regions. We examined the medial prefrontal cortex (mPFC), nucleus accumbens (NAc), and dorsal striatum (DS), which are regions associated with motivated behavior and ethanol consumption. Only *Tlr3* knockdown in the DS, predominately in neurons, decreased 2BC-EOD ethanol consumption, while also increasing the intoxicating effects of ethanol and diazepam and preventing development of AFT to ethanol. These effects corroborate and expand our previous findings in global *Tlr3* knockout mice and provide new evidence that neuronal TLR3 signaling within the DS regulates voluntary ethanol drinking.

2. Materials and methods

2.1. Generation of floxed Tlr3 (*Tlr3*$^{F/F}$) mouse line

CRISPR/Cas9 and Repair Template Production. Twenty nucleotide sgRNAs targeting Introns 5 and 6 were selected using the CRISPR Design Tool (Hsu et al., 2013). A sgRNA specific forward primer and a common overlapping reverse PCR primer (Table S1) were used to generate a T7 promoter containing individual sgRNA template, as described (Bassett et al., 2013). These DNA templates were transcribed *in vitro* using a MEGAshortscript Kit (Ambion, Inc., Austin, TX). The *Cas9* coding sequence was amplified from pX330 (Cong et al., 2013) using a T7 promoter containing forward and reverse primers (Table S1) and subcloned into pCR2.1-TOPO. This plasmid was digested with EcoRI and the ~ 4.3 kb fragment was *in vitro* transcribed and polyadenylated using the mMessage mMachine T7 Ultra Kit (Ambion). Following synthesis, the sgRNAs and *Cas9* mRNA were purified using the MEGAclear Kit (Ambion), ethanol precipitated, and resuspended in DEPC-treated water. Two 200-nucleotide, single-stranded DNA repair templates (Table S1) harboring loxP sites, restriction sites for genotyping, and sequences homologous to Introns 5 or 6 were purchased as Ultramer DNA (Integrated DNA Technologies, Coralville, IA). The oligos included 3 phosphorothioate linkages on each end (Renaud et al., 2016) and were symmetrically oriented with respect to the protospacer adjacent motif (PAM) and were complementary to the target strand.

Mouse Production. Tlr3 sgRNA#5 (50 ng/μl), *Tlr3* sgRNA#63 (50 ng/μL), *Cas9* mRNA (50 ng/μL), Intron 5 repair oligo (100 ng/μL), and Intron 6 repair oligo (100 ng/μL) were combined in embryo injection buffer (10 mM Tris, pH 7.4, 0.1 mM EDTA), aliquoted, and stored at −80 °C until microinjected. C57BL/6J one-cell embryos were collected from superovulated females and cultured in KSOM at 37 °C in 5 % CO_2/95 % air. Embryos were briefly transferred to M2 medium, and the nucleic acid mixture was injected into cytoplasm as described (Yang et al., 2014). Embryos that survived injection were transferred to the oviduct of day 0.5 postcoital psuedopregnant CD-1 recipient females.

Genotype Analysis. Pups resulting from manipulated embryos were screened for the loxP insertions in Introns 5 and 6 of the *Tlr3* gene by PCR amplification followed by restriction digestion. Briefly, a crude DNA extract was prepared from mouse tail tips or ear punches using 150 μL QuickExtract (Epicentre, Madison, WI). Amplicons from Introns 5 and 6 were PCR amplified with forward and reverse primers F1R1 and F2R2, respectively (Table S1). Intron 5 and 6 PCR products were digested with BamHI or EcoRI, respectively and analyzed by agarose gel electrophoresis. PCR amplicons were also analyzed by DNA sequencing.

Off-Target Analysis. The Benchling website (benchling.com) was used to identify predicted off-target sites for the sgRNA sequences. For *Tlr3* sgRNAs #5 and #63, the top 12 and 10 predicted off-targets, respectively (Table S2), were amplified from founder DNA and sequenced.

2.2. Animals

F2 heterozygous *Tlr3*$^{+/F}$ mice produced at the University of Pittsburgh were shipped to the University of Texas at Austin (UT Austin) to establish a breeding colony in the Animal Resources Center at UT Austin. Mice were kept in temperature- and humidity-controlled rooms with free access to food and water using a 12-h light/dark cycle (lights on at 7:00 a.m.). Male and female floxed *Tlr3* homozygous mice (*Tlr3*$^{F/F}$) mice and wild-type (WT) littermates were used for sequencing characterization and measurement of brain transcripts. *Tlr3*$^{F/F}$ male mice (2 to 3 months old) were used for behavioral experiments 4 weeks after recovery from regional brain injections of AAV5-CMV-GFP (Control) or AAV5-CMV-Cre-GFP (Cre). We used males because previous findings showed that 2BC-EOD ethanol consumption decreased only in *Tlr3* knockout males (Blednov et al., 2021). We also tested C57BL/6J male mice from our colony at UT Austin based on previous work showing that poly(I:C)-induced activation of TLR3 signaling increased 2BC-EOD ethanol consumption in male but not in female mice (Warden et al., 2019a, b). Mice were allowed to adapt to the testing rooms for about 1 week before testing. Separate groups of mice were tested in each behavioral procedure. After rotarod testing, the same mice were used for PCR analysis. Experiments were approved by the Institutional Animal Care and Use Committees at the University of Pittsburgh and UT Austin and complied with the ARRIVE guidelines and the National Institutes of Health Guide for the Care and Use of Laboratory Animals. The number of mice used in each experiment is reported in the figure captions.

Tlr3 floxed mice (C57BL/6J-*Tlr3*^{em1Geh}/J) will be available from The Jackson Laboratory Mouse Repository (JAX Stock No. 038754).

2.3. Tissue harvest and RNA isolation

The PFC was dissected from 5 males and 5 females of each homozygous genotype (*Tlr3*$^{F/F}$ and WT littermates). As described in the previous section, females were used for genotyping founders and to measure brain *Tlr3* transcripts but were not used for behavioral testing. The PFC and remaining brain tissue were flash-frozen in liquid nitrogen and stored at −80 °C until use. RNA was isolated using the MagMax 96

for Microarrays Total RNA Isolation kit (Invitrogen, Carlsbad, CA or Thermo Fisher Scientific, Waltham, MA). RNA concentration and purity were assessed using the Nanodrop 8000 (Thermo Fisher Scientific), and RNA integrity was assessed using the Agilent 2200 TapeStation (Agilent Technologies, Santa Clara, CA).

2.4. RT-PCR and sequence analysis of Tlr3 brain transcripts

A High-Capacity cDNA Reverse Transcription Kit with RNase Inhibitor (Thermo Fisher Scientific or Applied Biosystems, Waltham, MA) was used to synthesize cDNA from whole brain minus PFC RNAs (1 male of each homozygous genotype). Portions of the *Tlr3* transcript were PCR amplified from each sample using Platinum Taq DNA Polymerase High Fidelity (Invitrogen) and three overlapping primer sets (Table 1). Amplicons were electrophoresed in 2 % agarose, excised from the gel, and purified with a Zymoclean Gel DNA Recovery Kit (Zymo Research, Irvine, CA). Purified PCR products were sequenced in both directions using the amplification primers.

2.5. RT-qPCR measurement of Tlr3 transcripts in prefrontal cortex

PFC RNAs (5 males and 5 females of each homozygous genotype) were converted to cDNA using Applied Biosystem's High-Capacity cDNA Reverse Transcription Kit with RNase Inhibitor. qPCR was performed in triplicate 10-μL reactions using 10 ng cDNA and SsoAdvanced Probes Universal Supermix (Bio-Rad Laboratories, Hercules, CA). FAM-labeled TaqMan gene expression assays were used to amplify *Gusb* (Mm03003537_s1), *Gapdh* (Mm99999915_g1), and four exon junctions of the *Tlr3* transcript (Exon 3–4, Mm01207402_m1; Exon 4–5, Mm01207403_m1; Exon 5–6, Mm01207404_m1; Exon 6–7, Mm00446577_g1). Results were analyzed with CFX Maestro for Mac 1.1 (Bio-Rad Laboratories) using the single threshold Cq determination and ΔΔCq method (Livak and Schmittgen, 2001; Pfaffl, 2001). *Tlr3* expression levels were normalized to the reference genes *Gusb* and *Gapdh*.

2.6. Stereotaxic surgery and injection of AAV5 constructs

Tlr3$^{F/F}$ male mice were anesthetized with isoflurane and given bilateral intracranial injections (Truitt et al., 2016) into either the DS, NAc, or mPFC of AAV5-CMV-Cre-GFP or AAV5-CMV-GFP (5 x 10^{12} viral particles/mL) (University of North Carolina at Chapel Hill Virus Vector Core) using a Drummond NanoJect device (Drummond Scientific Co., Broomal, PA). Using the slow setting, 25–50 nL were dispensed at a time for a total of 350 nL, and the needle was left in place for 3–5 min after the final injection. For each brain region, we performed AAV injections on 2–3 separate cohorts of mice. Results were similar among the cohorts and experimental data were combined for each brain region. Two injection sites were tested in the DS to cover both the anterior and posterior portions of the central part of the DS. Stereotaxic coordinates relative to Bregma were as follows (DS, cohort 1: M/L: ±1.7 mm, A/P: +0.38 mm, D: 2.9 mm; DS, cohorts 2 and 3: M/L: ±1.8 mm, A/P: +1.18 mm, D: 2.9 mm; mPFC, cohorts 1 and 2: M/L: ±0.4 mm, A/P: +2.1 mm, D: +1.4 mm; NAc, cohorts 1 and 2: M/L: ±0.9 mm, A/P: +1.43 mm, D: −4.55 mm). After injections, there was at least a 4-week period for recovery and viral expression.

2.7. Immunofluorescence and colocalization of GFP with cell-type specific markers

Detection of Viral Infection. Tlr3$^{F/F}$ male mice that had undergone 2BC-EOD ethanol drinking were anesthetized with isoflurane, euthanized, and transcardially perfused with phosphate buffered saline (PBS), followed by 4 % paraformaldehyde (PFA) in PBS. Brains were extracted and post-fixed overnight in 4 % PFA at 4 °C, allowed to settle in 30 % sucrose, and then were frozen in O.C.T. Compound (Thermo Fisher Scientific). Frozen brains were sliced at 100-μm thickness on a Thermo Fisher HM525-NX cryostat and stored in PBS at 4 °C. Slices were then washed in PBS and blocked in 5 % normal goat serum and 0.3 % Triton-X for 60 min at room temperature. Slices were incubated overnight in primary antibody (Rabbit Polyclonal Anti-GFP, Santa Cruz, #A1305) in blocking solution at 4 °C. The next day, slices were washed in PBS and incubated in secondary antibody (Goat Anti Rabbit Alexa Fluor 488) for 2 h at room temperature, mounted with Fluoromount and imaged on a Zeiss Axio Zoom.V16 microscope (Zeiss, Oberkochen, Germany). See Fig. S1 for representative images.

Colocalization of GFP with Cell Markers. Tlr3$^{F/F}$ male mice were injected with AAV5-CMV-Cre-GFP or AAV5-CMV-GFP into the DS (M/L: ±1.8 mm, A/P: +1.18 mm, D: 2.9 mm). After 4 weeks, DS tissue was harvested, and slices prepared as described below. Samples were permeabilized for 25 min at room temperature in the dark (RT/D) with Permeabilization Buffer (0.05 % Triton X100, 0.05 % Tween 20 in 1x PBS), then blocked with 1x BlockAid™ (ThermoFisher, B10710) for 1 h at RT/D. Samples were stained with one of the following three combinations of antibodies overnight at 4 °C with gyration: A) Chicken anti-GFP (1:2000, ab13970, abcam, Boston, MA) + Rabbit anti-TLR3 (1:200, NB100-56571, Novus Biologicals, Centennial, CO) + Mouse anti-S100b (1:250, 66616–1, Proteintech, Rosemont, IL); B) Chicken anti-GFP (1:2000, ab13970, abcam) + Rabbit anti-TLR3 (1:200, NB100-56571, Novus Biologicals) + Mouse anti-NeuN (1:250, MAB377, EMD Millipore, Darmstadt, Germany); or C) Chicken anti-GFP (1:2000, ab13970, abcam) + Rabbit anti-TLR3 (1:200, NB100-56571, Novus Biologicals) + Rat anti-Iba1 (1:2000, ab283346, abcam). Samples were then washed three times with PBS-T (0.05 % Tween 20 in 1x PBS) for 25 min each at RT/D. Secondary staining was performed at RT/D for 2 h with the following combinations of antibodies plus NucBlue Reagent (1 drop/mL, ThermoFisher, R37605): A and B) Goat anti-Chicken AlexaFluor 488 (1:500, A11039, ThermoFisher) + Goat anti-Rabbit AlexaFluor 568 (1:500, A11040, ThermoFisher) + Goat anti-Mouse IgG1 AlexaFluor 647 (1:500, A21240, ThermoFisher); C) Goat anti-Chicken AlexaFluor 488 (1:500, A11039, ThermoFisher) + Goat anti-Rabbit AlexaFluor 568 (1:500, A11040, ThermoFisher) + Donkey anti-Rat AlexaFluor 647 (1:500, A78947, ThermoFisher). Fully labeled samples were washed three times with PBS-T (0.05 % Tween 20 in 1x PBS) for 25 min each at RT/D. Samples were floated onto microscope slides, mounted with Aqua-Poly/Mount (18606–20, Polysciences, Warrington, PA), cover slipped with Number 1.5 coverslips, and allowed to cure overnight at 4 °C before imaging. A Nikon A1R laser scanning confocal system equipped with a LUN-V 6-line laser unit (405 nm, 488 nm, 561 nm, 640 nm), Plan Apo λ 20x (Air) objective (NA − 0.75; WD − 1 mm), and a Plan Fluor DIC 40x (Oil) objective (NA − 1.3; WD − 0.24 mm) was used to collect Z-stack images at 1024x1024 resolution. The ability of AAV5 to transfect cells was determined by object-based colocalization

Table 1
Primers used for RT-PCR and Sequencing of *Tlr3* Brain Transcripts.

Forward Primer	Forward Primer Sequence	Reverse Primer	Reverse Primer Sequence	Amplicon Length
F2	AGGTTGACGCACCTGTTCTC	R2	GTTCTTCACTTCGCAACGCA	737
F3	GGGTCCAACTGGAGAACCTC	R4	CTTGAAAACCCCGACTGGGA	1250
F5	GGCTGTCTCACCTCCACATC	R7	GGCCTTTCTGAGCTACACAGT	1393

PCR primers were designed using MacVector v15.5.3 (MacVector, Inc., Apex, NC). Primer specificity was evaluated with the basic local alignment search tool (BLAST, NCBI, Bethesda, MD). Amplicons were sequenced and aligned to the reference sequence (NM_126166) using the "Align to Reference" tool of MacVector.

analysis of GFP with cell-type specific markers in images of the DS. These measurements were performed on three maximal intensity projection images per mouse using Fiji-ImageJ2 v2.14.0/1.54f (Schindelin et al., 2012). Three dimensional images were generated by importing image stacks into Imaris v10.1 software (Andor Technology, Concord, MA).

2.8. RT-qPCR measurement of Tlr3 transcripts

Tissue Harvest and RNA Isolation. Brains were isolated from *Tlr3*$^{F/F}$ male mice 4–8 weeks after injection of AAV constructs into either the DS, mPFC, or NAc. Mice that received DS injections were anesthetized with isoflurane and euthanized, and their brains were flash frozen in Optimal Cutting Temperature (OCT) Compound (Thermo Fisher Scientific) in brain molds. Mice that received mPFC or NAc injections were sacrificed by cervical dislocation and decapitated without anesthesia, and the brains were flash frozen in liquid nitrogen and later embedded in OCT media in isopentane on dry ice. Brains were stored at −80 °C and later transferred to a cryostat set at −6 °C 1 h before sectioning. All equipment used in sectioning, micropunching, and RNA extraction was treated with RNaseZap (Sigma Aldrich, St. Louis) to prevent RNA degradation. Brains were sliced at 300-μm thickness on a Thermo Fisher HM525-NX cryostat, and slices were mounted on charged microscope slides precooled on dry ice. Tissue punches (DS and NAc: 1.5 mm diameter; mPFC: 0.75 mm diameter) were collected from slices with visible GFP fluorescence. Six tissue punches were collected from each animal. GFP fluorescence was visualized using a GFP illuminating flashlight (Bluestar Flashlight system, NightSea, Hatfield, PA). RNA was isolated using an RNeasy Mini Kit (Qiagen, Hilden, Germany) according to the manufacturer's protocol. RNA concentration and purity were assessed using a Nanodrop 8000 (Thermo Fisher Scientific).

RT-qPCR Analysis. cDNA was generated from DS, mPFC, or NAc RNA using a High-Capacity cDNA Reverse Transcription Kit (Invitrogen) and analyzed on a QuantStudio 12 K Flex Real-Time PCR System using PrimeTime Gene Expression Master Mix (Integrated DNA Technologies, Inc., Coralville, IA). TaqMan assays were used to target four exon junctions of the *Tlr3* transcript as described earlier for PFC samples. Expression levels were calculated by the ΔΔCt method and normalized to *Gapdh*.

2.9. Two-Bottle Choice, Every-Other-Day ethanol drinking

The 2BC-EOD drinking procedure was developed to induce high voluntary ethanol consumption in mice (Melendez, 2011; Rosenwasser et al., 2013). We routinely use this procedure in our studies of genetic or pharmacological manipulations in mice (Blednov et al., 2017; Blednov et al., 2022; Blednov et al., 2021; Warden et al., 2019a). Here, we tested 2BC-EOD ethanol drinking in ethanol-naïve *Tlr3*$^{F/F}$ male mice after recovery from stereotaxic surgeries to inject AAV5-CMV-Cre-GFP or control constructs into different brain regions. Mice were singly housed throughout the duration of the procedure, and drinking sessions were conducted every-other-day for 24 h in the home cage. On ethanol drinking days, mice had access to two bottles, one containing 15 % (v/v) ethanol, and one containing water. On non-ethanol drinking days, only water was available. Measurements of ethanol intake, preference for ethanol, and total fluid intake were averaged over two drinking days with different bottle positions to eliminate side preference.

2.10. Rotarod ataxia

Before rotarod testing, *Tlr3*$^{F/F}$ male mice that had recovered from injections of AAV5-CMV-Cre-GFP or AAV5-CMV-GFP into the DS were placed on a fixed-speed (10 rpm) rotarod to become accustomed to the task (Economex; Columbus Instruments, Columbus, OH). Most mice balance on the rotarod for 60 s after their first placement, and for any mouse that does not, we repeat the exposure a second or third time. Drug injections began 15 min later. Every 15 min after i.p. injection of ethanol (2 g/kg) or diazepam (7 mg/kg), each mouse was placed on the rotarod and latency to fall was measured until the mouse could once again remain on the rotarod for 60 s. Ethanol (100 % stock, Aaper Alcohol and Chemical, Shelbyville, KY) was freshly prepared in 0.9 % saline (20 %, v/v) for i.p. injection. Diazepam (Sigma-Aldrich, St. Louis, MO) was freshly prepared in 0.9 % saline with 3–4 drops of Tween-80 and injected i.p. at 0.1 mL/10 g body weight.

In a separate experiment, we tested poly(I:C) in C57BL/6J male mice to measure the effect of systemic TLR3 activation on ethanol-induced ataxia. Poly(I:C) HMW (InvivoGen, San Diego, CA) was freshly prepared as described previously (Cunningham et al., 2007). After C57BL/6J male mice demonstrated the ability to balance on the rotarod for 60 s, they received i.p. injections of saline or 5 mg/kg poly(I:C) 3 h before injection of 2 g/kg ethanol. Latency to fall was measured as described above. This dose and time were chosen based on the increased 2BC-EOD ethanol consumption in C57BL/6J male mice and increased *Tlr3* and other TRIF-dependent immune transcripts in the brain 3-h after poly(I:C) administration (Warden et al., 2019a).

2.11. Acute functional tolerance

AFT to ethanol-induced ataxia was measured using the two-dose method (Erwin and Deitrich, 1996) in *Tlr3*$^{F/F}$ male mice after recovery from DS injections of viral constructs. After becoming accustomed to the rotarod task, mice were injected with ethanol (1.75 g/kg, i.p.) and placed back on the rotarod until they fell off. Mice were tested in 5-min intervals until they regained the ability to balance on the rotarod for 60 s. Once this was achieved (t1), a *retro*-orbital blood sample was collected to measure blood ethanol concentration (BEC1). Mice were then immediately given a second ethanol injection (2 g/kg, i.p.). After losing the ability to remain on the rotarod, mice were tested in 5-min intervals until they regained the ability to balance for 60 s (t2). Then a second blood sample was collected to measure BEC2. AFT was defined as the difference in BEC at t2 and t1 (BEC2 - BEC1).

To measure BECs, *retro*-orbital blood samples (~20 μL) were collected in capillary tubes and centrifuged for 6 min at 3,100 x g using a Haematospin 1400 centrifuge (Analox Instruments, London, UK). Plasma samples were stored at − 20 °C until BECs were determined in 5-μL aliquots using an AM1 Alcohol Analyzer (Analox Instruments). The machine was calibrated every 15 samples using an industry standard, and BECs were determined using commercially available reagents according to the manufacturer's instructions. Samples were averaged from duplicate runs and expressed as mg/dL.

2.12. Statistical analysis and study design

Animals were assigned randomly to various experimental groups, and data are reported as mean ± S.E.M values. The number of mice used in each study are reported in the figure captions. For each brain region, separate cohorts of mice underwent 2BC-EOD ethanol drinking after injection of viral constructs, and the data were combined. Statistical analysis was performed using Prism 10.2 (GraphPad Software, Inc., La Jolla, CA). Data were analyzed by student's *t*-tests or by two-way ANOVA or two-way ANOVA with repeated measurements and Bonferroni or Holm-Šidák's multiple comparisons *post-hoc* tests. To measure development of AFT, Wilcoxon signed rank tests were used to compare experimental data with a theoretical median of 0.

3. Results

3.1. Tlr3$^{F/F}$ mouse production

To manipulate TLR3 signaling in discrete brain regions, we used CRISPR/Cas9 genome editing technology to generate a floxed *Tlr3* mouse line. The CRISPR/Cas9 RNA guided nuclease and single stranded

DNA oligonucleotides were used to insert loxP and restriction sites in Introns 5 and 6 of the *Tlr3* gene as illustrated in Fig. 1A. The loxP sequence in Intron 5 is located 123 bp upstream of Exon 6. The loxP sequence in Intron 6 is located 43 bp downstream of Exon 6. A total of 18 founder animals were produced from embryos injected as described in the methods; one founder (mouse #4773, a female) harbored a correctly floxed Exon 6 and appeared to be homozygous. The Intron 5 insertion adds a BamHI restriction site along with loxP and results in BamHI fragments of 153 and 231 bp (data not shown). In contrast, the WT Intron 5 amplicon (344 bp) is not digested with BamHI and was not observed in this mouse. The Intron 6 insertion adds an EcoRI restriction site along with loxP and results in EcoRI fragments of 145 and 257 bp. In contrast, the WT Intron 6 amplicon (362 bp) is not digested with EcoRI; this WT fragment was not observed in this mouse. PCR/DNA sequence analysis of these amplicons confirmed the expected sequences (Fig. 1B and C) except for deletion of a single G 6 bp upstream of the Intron 6 insertion. To ensure that there were no large genomic indels/rearrangements near the loxP insertions, genomic DNA from founder #4773 was digested with BamHI, EcoRI, or both enzymes and analyzed by Southern blot analysis with an Exon 6 specific probe (data not shown). This analysis revealed that mouse #4773 was homozygous floxed with no gross indels/rearrangements at the *Tlr3* locus. None of the predicted top 12 *Tlr3* sgRNA#5 off-target sites in founder #4773 were mutated. Similarly, none of the 10 predicted top off-target sites for *Tlr3* sgRNA#63 were mutated.

Founder #4773 was mated to a C57BL/6J male to establish the line reported here. All offspring were genotyped for the loxP insertions in Introns 5 and 6 using the PCR/restriction fragment length polymorphism approach illustrated in Fig. 1A. From 8 offspring derived from this founder, two were heterozygous for both loxP insertions. The Intron 5 and 6 amplicons from both were sequenced to verify the fidelity of the floxed locus. These two heterozygous F1 males were subsequently mated to WT C57BL/6J females to produce the F2 heterozygous mice that were shipped to UT Austin for breeding, characterization, and behavioral testing.

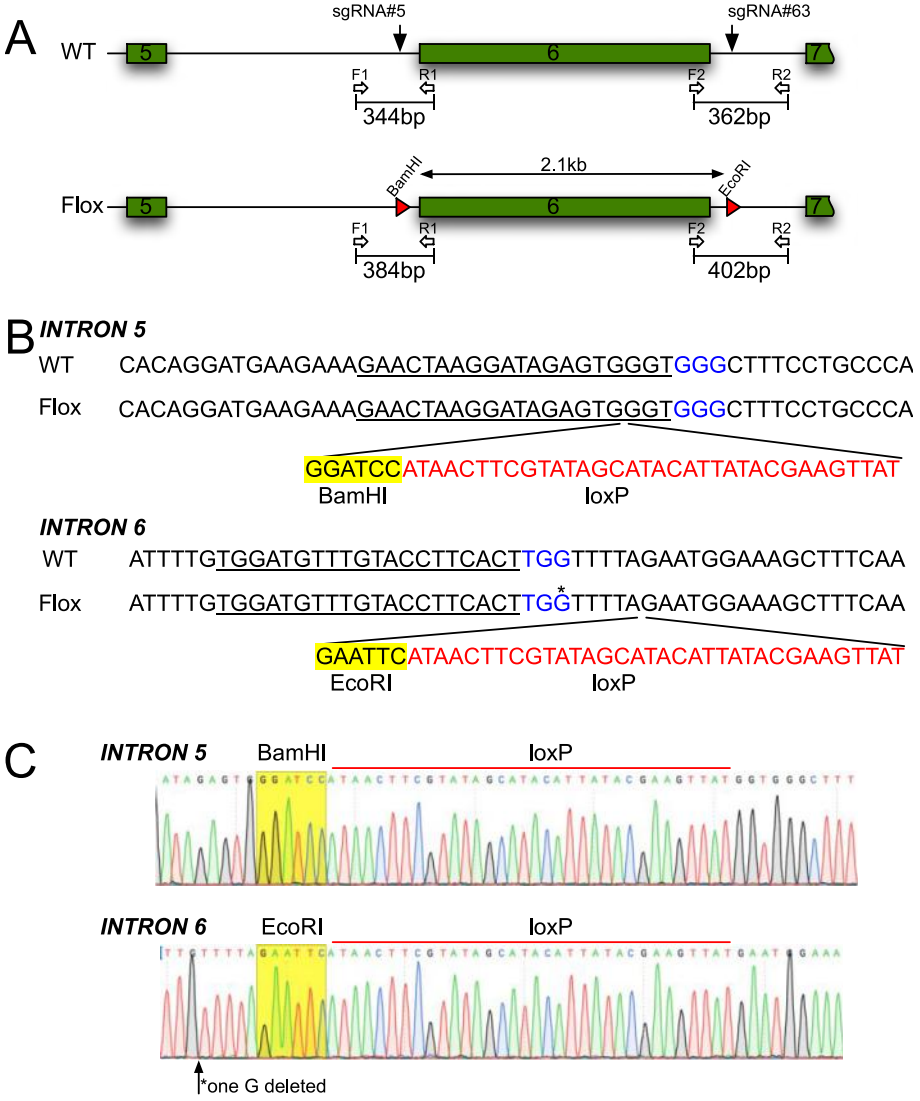

Fig. 1. *Tlr3* floxed mouse strategy. (A) Diagrammatic representation of wild-type (WT) and floxed *Tlr3* loci. Shown are the PCR primers (F1, R1, F2, and R2) and amplicon sizes that were used for genotype analysis. Note: Introns and exons are not drawn exactly to scale. **(B)** Partial *Tlr3* WT and floxed mouse DNA sequence for Introns 5 and 6. The sgRNA sequence (underlined), CRISPR protospacer adjacent motif (blue text), loxP sequence (red text), and added restriction sites (highlighted in yellow) are also marked. **(C)** DNA sequencing chromatograms from founder mouse #4773. Note: The * over the G in panel B on the Intron 6 flox sequence is the G deleted in the founder mouse line as shown in the chromatogram. (For interpretation of the references to colour in this figure legend, the reader is referred to the web version of this article.)

3.2. RT-PCR and sequence analysis of Tlr3 brain transcripts

Next, we performed functional analysis of the *Tlr3* locus. RT-PCR products spanning most of Exon 2 through the beginning of Exon 7 (which includes the entire coding sequence) were sequenced in whole brain minus PFC from one WT and one homozygous floxed male (Fig. S2). All samples produced the expected sequence with no additional alterations.

3.3. Tlr3 mRNA levels are not altered by LoxP insertions

Four TaqMan assays targeting different exon junctions (3–4, 4–5, 5–6, and 6–7) of the *Tlr3* transcript were used to compare expression levels in the PFC from untreated male and female WT and $Tlr3^{F/F}$ mice (Fig. S3). Data were normalized to reference genes *Gusb* and *Gapdh*, which exhibited low variability (Cq range < 0.6) across all samples. Two-way ANOVA showed a significant effect of sex in two assays ($p = 0.0413$ for Exon 4–5 and 0.0399 for Exon 6–7), but *post-hoc* analysis by Holm-Šidák's multiple comparisons test indicated the effects were not significant ($p > 0.1368$ for all comparisons). Thus, for each assay, males and females were combined. There were no genotype differences in *Tlr3* expression in any of the assays ($p > 0.1$, two-tailed *t*-tests), indicating expression levels were not affected by the loxP insertions for Cre recombinase (Fig. S3).

3.4. Validation of Tlr3 knockdown

To verify that Cre recombinase decreased *Tlr3* mRNA expression in each brain region studied, we used RT-qPCR to measure *Tlr3* mRNA in tissue punches from $Tlr3^{F/F}$ male mice 4–8 weeks after injections of an adeno-associated virus expressing Cre recombinase (AAV5-CMV-Cre-GFP) or GFP as a control (AAV5-CMV-GFP). GFP expression in each sample was confirmed visually prior to tissue punching. RT-qPCR was performed using the same four TaqMan assays used to measure *Tlr3* expression in untreated mice as described above. Assays were designed to span junctions 5–6 and 6–7 of floxed Exon 6 and junctions 3–4 and 4–5 that are upstream of the floxed exon. In the DS, Cre recombinase-treated mice showed significant (>50 %) *Tlr3* knockdown in assays targeting the floxed exon (Exon 5–6: $t(18) = 6.284$, $p < 0.0001$; Exon 6–7: $t(18) = 7.534$, $p < 0.0001$, unpaired *t*-tests) and small increases in upstream exons (Exon 3–4: $t(18) = 2.819$, $p < 0.05$; Exon 4–5: $t(18) = 2.921$, $p < 0.01$, unpaired *t*-tests) (Fig. S4). In the mPFC and NAc, transcripts containing the floxed Exon 6 were also significantly decreased in Cre-treated animals compared with controls (mPFC: Exon 5–6, $t(10) = 14.67$, $p < 0.0001$; Exon 6–7, $t(10) = 18.05$, $p < 0.0001$; NAc: Exon 5–6, $t(10) = 20.83$, $p < 0.0001$; Exon 6–7, $t(10) = 22.60$, $p < 0.0001$). Brain transcripts containing unfloxed Exons 3–4 and 4–5 were not significantly altered by Cre treatment in these regions. Deletion of Exon 6 and the resulting frameshift in Exon 7 is predicted to delete 693 of the 905 amino acids of the TLR3 protein resulting in a null allele. Significant reduction in Exon 6 containing *Tlr3* transcripts following Cre-mediated recombination would be expected to produce corresponding decreases in TLR3 protein expression.

3.5. Tlr3 knockdown in dorsal striatum decreases ethanol consumption

After validation studies in mouse brain, we injected $Tlr3^{F/F}$ mice with AAV5-CMV-GFP or AAV5-CMV-Cre-GFP into either the DS, mPFC, or NAc. Following a 4-week recovery period, male mice underwent 2BC-EOD ethanol drinking, the same procedure that showed decreased drinking in global *Tlr3* knockout male mice (Blednov et al., 2021).

We tested two injection sites in the anterior and posterior portions of the central part of the DS. *Tlr3* knockdown in both areas reduced 2BC-EOD ethanol drinking (Fig. 2). Compared with mice injected with control virus, ethanol intake was lower in mice that received AAV5-CMV-Cre-GFP [$F_{treatment}$ (1, 54) = 5.292, $p = 0.0253$; F_{time} (1, 54) = 5.184, $p = 0.0006$; $F_{treatment\ x\ time}$ (6, 324) = 1.838, $p = 0.0912$], while the effect of treatment on preference for ethanol was of borderline significance [$F_{treatment}$ (1, 54) = 3.320, $p = 0.0740$; F_{time} (6, 324) = 5.674, $p = 0.0002$; $F_{treatment\ x\ time}$ (6, 324) = 1.957, $p = 0.0714$]. Total fluid intake was not altered in Cre-expressing mice.

In contrast with the DS, *Tlr3* knockdown in the mPFC or NAc did not alter ethanol consumption. During the 2BC-EOD procedure, ethanol intake increased across the drinking days [mPFC: $F(5, 210) = 10.28$, $p < 0.0001$; NAc: $F(7, 189) = 8.458$, $p < 0.0001$], as did preference for ethanol [mPFC: $F(5, 210) = 13.91$, $p < 0.0001$; NAc: $F(7, 189) = 7.219$, $p = 0.0081$]. However, there was no significant effect of Cre treatment in the mPFC or NAc on any drinking parameter (Fig. 3).

3.6. Tlr3 knockdown in dorsal striatum prolongs ataxia by ethanol and diazepam

We next examined the acute effects of ethanol on ataxia in male mice after *Tlr3* knockdown in the DS. We also tested diazepam based on our work showing that global *Tlr3* knockout male mice were more sensitive to both ethanol- and diazepam-induced rotarod ataxia compared with their WT littermates (Blednov et al., 2021). Like the global knockouts, $Tlr3^{F/F}$ mice with Cre expressed in the DS showed prolonged recovery from ataxia induced by 2 g/kg ethanol [$F_{time\ x\ treatment}$ (8, 136) = 97.96, $p < 0.0001$] or by 7 mg/kg diazepam [$F_{time\ x\ treatment}$ (6, 102) = 44.35, $p < 0.0001$] compared with control mice (Fig. 4A and C). There was a significant increase in area over the recovery curve after injection of ethanol [$t(17) = 20.33$, $p < 0.0001$; Fig. 4B] or diazepam [$t(17) = 10.48$, $p < 0.0001$; Fig. 4D] in Cre-expressing vs. control mice (unpaired *t*-tests).

These results suggest a potential functional relationship between

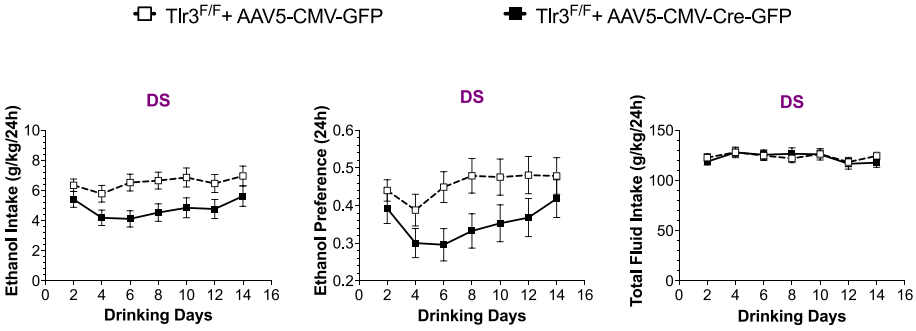

Fig. 2. *Tlr3* knockdown in the dorsal striatum decreases ethanol consumption and preference, but not total fluid intake, in a 2BC-EOD drinking procedure. Four weeks after injections of AAV5-CMV-GFP (n = 27) or AAV5-CMV-Cre-GFP (n = 29) into the dorsal striatum (DS), $Tlr3^{F/F}$ male mice underwent two-bottle choice, every-other-day (2BC-EOD) ethanol (15 % v/v) drinking. Graphs represent combined data from two DS injection sites (M/L: ±1.7 mm, A/P: +0.38 mm, D: 2.9 mm and M/L: ±1.8 mm, A/P: +1.18 mm, D: 2.9 mm).

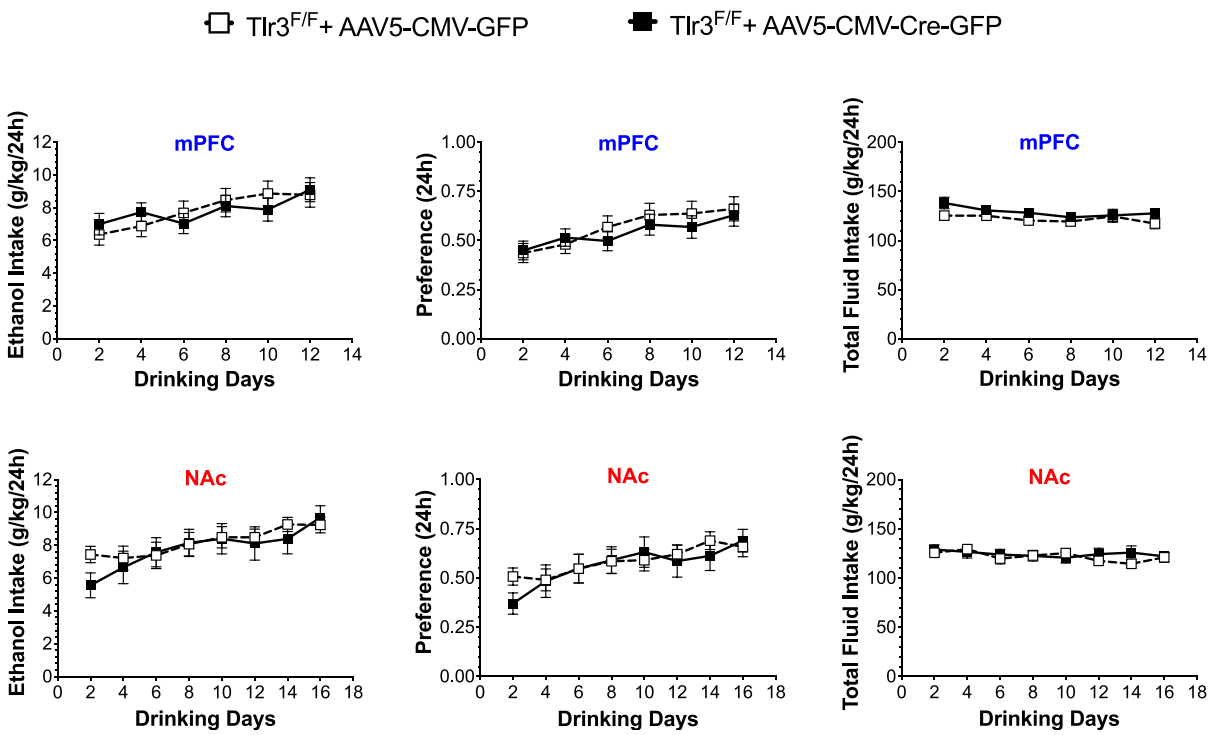

Fig. 3. *Tlr3* knockdown in the medial prefrontal cortex or nucleus accumbens does not alter voluntary ethanol drinking. Four weeks after injections of AAV5-CMV-GFP (Control) or AAV5-CMV-Cre-GFP (Cre) into the medial prefrontal cortex (mPFC) or nucleus accumbens (NAc), *Tlr3*$^{F/F}$ male mice underwent two-bottle choice, every-other-day ethanol (15 % v/v) drinking. mPFC: Control, n = 22; Cre, n = 22; NAc: Control, n = 15; Cre, n = 14. Two different cohorts of mice were studied per region and the data combined.

TLR3 signaling and ethanol-induced ataxia. If there is such a relationship, we hypothesized that because TLR3 knockdown increased sensitivity to the ataxic effects of ethanol, then TLR3 activation would have the opposite effect. To test this, we examined the effect of 5 mg/kg poly (I:C) on ethanol-induced ataxia in C57BL/6J males and found that it accelerated recovery from ataxia by 2 g/kg ethanol [$F_{\text{time x treatment}}$ (6, 132) = 7.341, $p < 0.0001$] and produced a significant decrease in area over the ethanol recovery curve [t(22) = 5.977, $p < 0.0001$] (Fig. 5). Thus, TLR3 activation shortened, while TLR3 knockdown in the DS prolonged, the ataxic effects of ethanol.

3.7. *Tlr3* knockdown in dorsal striatum prevents acute functional tolerance to ethanol

Differences in time to recover from drug-induced ataxia suggest that Cre-expressing and control *Tlr3*$^{F/F}$ mice differ in their development of AFT. AFT is behavioral tolerance to ethanol that occurs within an individual test session and can be measured by the time taken to recover from rotarod ataxia. We previously found that decreased ethanol consumption in global *Tlr3* knockout mice was associated with decreased AFT to ethanol (Blednov et al., 2021). Here, we examined *Tlr3*$^{F/F}$ male mice after striatal injections of AAV5-CMV-GFP (Control) or AAV5-CMV-Cre-GFP (Cre). The times to recover from motor impairment after the first (1.75 g/kg) and second ethanol (2 g/kg) injections were longer in Cre-expressing than in control mice [$F_{\text{recovery time x treatment}}$ (1, 18) = 117.3, $p < 0.0001$] (Fig. 6A).

After both injections, BECs at the time of recovery were higher in control than in Cre-treated *Tlr3*$^{F/F}$ mice [$F_{\text{recovery time x treatment}}$ (1, 18) = 21.03, p = 0.0002] (Fig. 6B). Despite significantly lower BECs in the Cre group, they took longer to recover. The difference in recovery time between the second and first ethanol injections was greater in the Cre group [t(18) = 10.83, $p < 0.0001$, unpaired *t*-test] (Fig. 6C). Control mice developed AFT (BEC2 - BEC1) to the ataxic effect of ethanol (p = 0.002 compared with a theoretical median of 0, Wilcoxon test) (Fig. 6D). However, Cre-expressing mice did not (p = 0.5703), indicating that *Tlr3* knockdown in the DS prevents development of AFT to ethanol. AFT was significantly reduced in Cre-expressing mice [t(18) = 4.586, p = 0.0002, unpaired *t*-test].

3.8. *Tlr3* knockdown in neurons in dorsal striatum

To determine if *Tlr3* knockdown in a particular cell type in the DS was responsible for the behavioral effects, we examined colocalization of GFP with cell-type specific markers (Fig. 7). In mice transfected with AAV5-CMV-Cre-GFP, 87 ± 2 % (n = 4 mice) of all GFP-positive cells expressed the neuronal marker NeuN (Fig. 7A). In contrast, less than 5 % of GFP-positive cells also expressed the astrocytic marker S100B (Fig. 7B) and less than 1 % expressed the microglial marker Iba1 (Fig. 7C). TLR3 immunoreactivity was reduced in AAV5-CMV-Cre-GFP transfected DS compared with AAV5-CMV-Control-GFP transfected DS (Fig. 7D and E). Fig. 7F is a 3-D reconstruction showing colocalization of TLR3, GFP, and NeuN immunoreactivity in a striatal neuron from a mouse injected with AAV5-CMV-Control-GFP. These results indicate that AAV5-CMV-Cre-GFP effectively reduced TLR3 primarily in DS neurons.

4. Discussion

We used CRISPR/Cas9 genome editing to produce floxed *Tlr3* mice (available from The Jackson Laboratory Mouse Repository, Stock No. 038754) and provided functional validation of the *Tlr3* loci in mouse brain. In the absence of Cre recombinase, *Tlr3*$^{F/F}$ mice and WT littermates contained similar amounts of *Tlr3* transcripts in the PFC, indicating that the engineered loxP insertion sites for Cre recombinase did not interfere with gene expression, splicing, or decay. Using this new mouse model, we provide evidence that discrete manipulation of TLR3 in the adult brain regulates voluntary ethanol consumption. Previous studies have relied on global *Tlr3* knockout or systemic treatment with

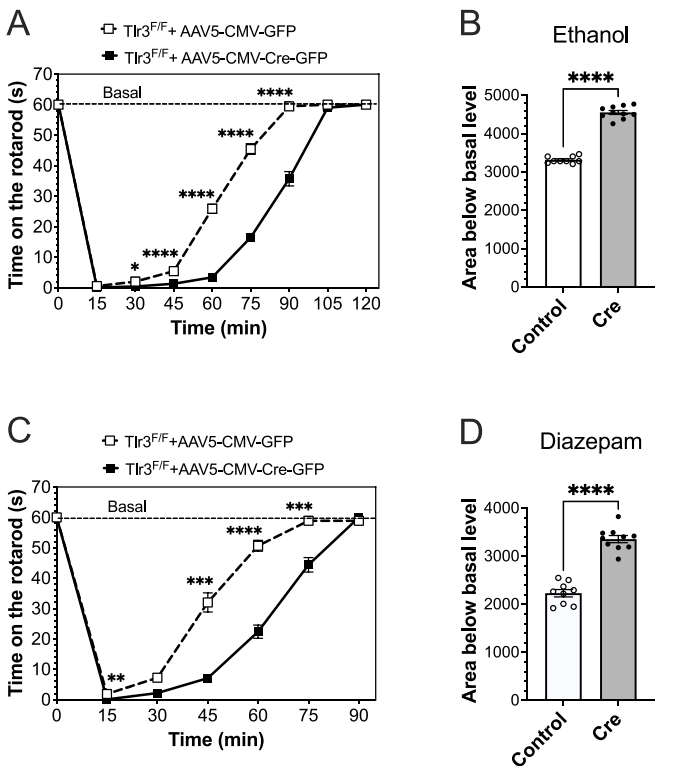

Fig. 4. *Tlr3* knockdown in the dorsal striatum prolongs recovery from ethanol- and diazepam-induced ataxia. Time on the rotarod after injection of **(A)** ethanol (2 g/kg, i.p.) or **(C)** diazepam (7 mg/kg, i.p.) in *Tlr3*$^{F/F}$ male mice 4 weeks after dorsal striatal injections of AAV5-CMV-GFP (Control, n = 9) or AAV5-CMV-Cre-GFP (Cre, n = 10) (*p < 0.05, **p < 0.01, ***p < 0.001, ****p < 0.0001 compared with the corresponding saline control timepoint (Bonferroni multiple comparisons *post-hoc* tests). Area below basal level and above the recovery curve after **(B)** ethanol or **(D)** diazepam (****p < 0.0001, unpaired *t*-tests).

poly(I:C), both of which can have peripheral immune effects that impact behavior, so it was important to determine if TLR3 signaling in the brain directly regulates ethanol drinking. Of the three brain regions examined, only *Tlr3* knockdown in the DS reduced 2BC-EOD ethanol drinking. The effect on drinking corroborates our previous findings in global *Tlr3* knockout male mice using the same 2BC-EOD procedure (Blednov et al., 2021). In both studies (global knockout and DS-specific knockdown), the decreases in ethanol consumption were associated with prolonged ethanol-induced ataxia and absence of AFT to ethanol. There were no differences in blood ethanol clearance in global knockout mice that could account for these effects (Blednov et al., 2021). Furthermore, in mice with knockdown of *Tlr3* in the DS, the time to recover the ability to remain on the rotarod after ethanol injections was slightly longer but occurred at slightly lower BECs during the AFT test. This result is consistent with these mice having similar blood ethanol clearance as controls but increased sensitivity to ethanol.

Global and DS-specific *Tlr3* knockdown also prolonged recovery from diazepam-induced ataxia, indicating a role for GABAergic signaling in TLR3 responses. TLR3 was mainly colocalized with DS neurons and based on the degree of viral transfection in different cell types, *Tlr3* would be primarily knocked down in neurons. Most neurons in the striatum and its projection areas use GABA as a transmitter and express glutamic acid decarboxylate, the rate limiting enzyme in the synthesis of GABA (Lindefors, 1993). Our results raise the question of how TLR3, an endosomal receptor, could be associated with $GABA_A$ receptor function at the cell surface. The number and membrane stability of $GABA_A$ receptors is regulated by expression of the intracellular ubiquitin-like protein PLIC-1, a key component of $GABA_A$ receptor trafficking (Mele et al., 2019; Saliba et al., 2008). PLIC-1 has also been reported to regulate TLR3-TRIF signaling *in vitro* (Biswas et al., 2011). This raises the possibility of co-regulation of $GABA_A$ and TLR3-dependent responses by a common intracellular mediator. We note that future studies of GABAergic synaptic transmission and $GABA_A$ receptor subunit expression in DS cells after *Tlr3* knockdown are needed to explore a possible association between $GABA_A$ receptor function and TLR3 responses.

In contrast to genetic deletion or knockdown, repeated activation of TLR3 using poly(I:C) increased ethanol intake in different rodent drinking models, including the 2BC-EOD procedure (Gano et al., 2022; Lovelock et al., 2022; Randall et al., 2019; Warden et al., 2019a). A TLR3/dsRNA complex inhibitor reduced poly(I:C)-mediated ethanol consumption, indicating the escalation in drinking was at least partially dependent on TLR3 signaling in C57BL/6J male mice (Warden et al., 2019a). In the current study, poly(I:C) accelerated recovery from ethanol-induced ataxia in these mice. If activation of TLR3 signaling decreases the intoxicating effects of ethanol, this could explain the ability of poly(I:C) to increase 2BC-EOD drinking in C57BL/6J males (Warden et al., 2019a). Collectively, our studies of activating or inhibiting TLR3 signaling showed that these manipulations produce opposite effects on intoxication, AFT to ethanol, and ethanol consumption in

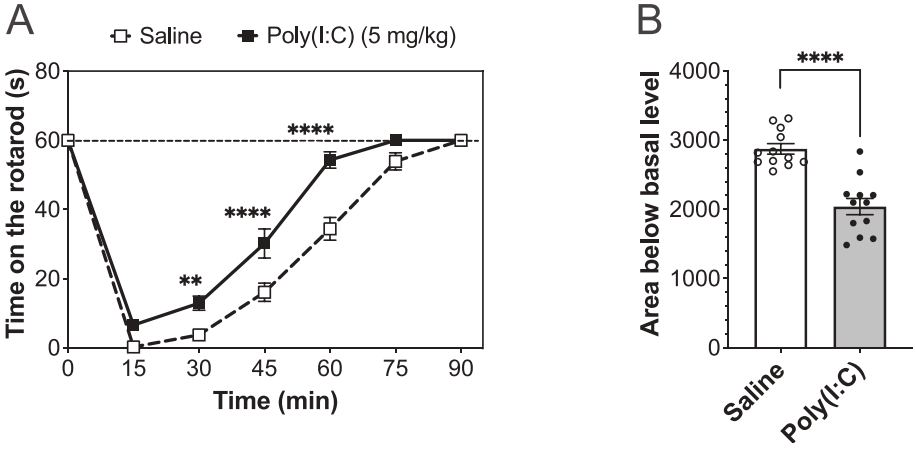

Fig. 5. Poly(I:C) accelerates recovery from ethanol-induced ataxia in C57BL/6J male mice. (A) Time on the rotarod after injection of ethanol (2 g/kg, i.p.) in C57BL/6J male mice pretreated 3 h earlier with i.p. injections of saline or 5 mg/kg poly(I:C) (n = 12 per group) (**p < 0.01, ****p < 0.0001 compared with the corresponding saline control timepoint, Bonferroni multiple comparisons *post-hoc* test). **(B)** Area below basal level and above the recovery curve after ethanol injection (****p < 0.0001, unpaired *t*-test).

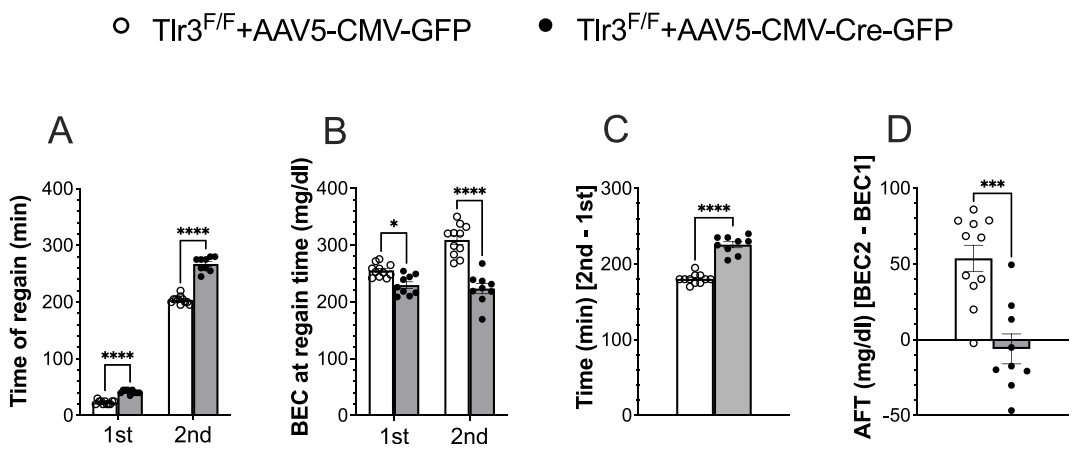

Fig. 6. *Tlr3* knockdown in dorsal striatum prevents development of acute functional tolerance to ethanol. Four weeks after dorsal striatal injections of AAV5-CMV-GFP (n = 11) or AAV5-CMV-Cre-GFP (n = 9), *Tlr3*$^{F/F}$ male mice underwent rotarod testing. **(A)** Time to regain the ability to remain on the rotarod for 60 s after the first (1.75 g/kg, i.p.) and second (2 g/kg, i.p.) ethanol injections (****p < 0.0001, Bonferroni multiple comparisons *post-hoc* tests). **(B)** Blood ethanol concentrations (BECs) measured at the time of regaining motor function after the first and second ethanol injections (*p < 0.05, ****p < 0.0001, Bonferroni multiple comparisons *post-hoc* tests). **(C)** Difference in recovery time between the second and first ethanol injections (****p < 0.0001, unpaired *t*-test). **(D)** Acute functional tolerance (AFT) to ethanol measured as the difference in BECs after the two ethanol injections (BEC2 - BEC1) (***p = 0.0002, unpaired *t*-test).

male mice. For example, systemic TLR3 activation shortened, while TLR3 knockdown (global or DS-specific) prolonged, the intoxicating effects of ethanol. This is consistent with the effects of these treatments on ethanol consumption in male mice, where activation of TLR3 signaling increases 2BC-EOD drinking (Warden et al., 2019a), while TLR3 knockdown (global or DS-specific) decreases 2BC-EOD drinking (Blednov et al., 2021). Future studies will determine if poly(I:C)-mediated effects on recovery from ethanol ataxia, AFT, or ethanol consumption are reversed by *Tlr3* knockdown in the DS.

Chronic ethanol exposure also regulates expression of TLR3 in mouse brain. For example, increases in brain mRNA and protein expression of TLRs 2, 3, and 4 were found in chronic ethanol-treated mice (Crews et al., 2013). These mRNAs and transcripts of the TRIF-dependent pathway also increased in the mPFC of male mice after chronic 2BC-EOD ethanol consumption (McCarthy et al., 2018). In addition, repeated treatment with poly(I:C) during chronic 2BC-EOD drinking upregulated TRIF-dependent pathway components in the mPFC and were positively correlated with increased ethanol consumption in male mice (Warden et al., 2019a). Similar effects have been observed in human subjects with AUD. For example, increases in TLR 2, 3, and 4 immunoreactivities in postmortem orbitofrontal cortex from individuals with AUD were positively correlated with lifetime alcohol consumption (Crews et al., 2013). However, we found that knockdown of *Tlr3* in the PFC does not alter drinking behavior in mice. Considering our current and prior findings that GABAergic signaling is regulated by TLR3 (Blednov et al., 2021), it is possible that the effects of *Tlr3* knockdown specifically in the DS are related to striatal GABAergic pathways that have been shown to drive alcohol consumption (Cheng et al., 2017). Our results showing TLR3 colocalized with neurons and viral transfection occurring predominantly in DS neurons lend support to a neuronal mechanism.

We propose that activation of TLR3 signaling in the DS helps drive ethanol consumption and that this pathway could be a potential target to reduce excessive drinking. The DS is implicated in the progression from recreational to compulsive ethanol use and in reinforcement (Clarke and Adermark, 2015). An extensive literature has linked functional changes in the striatum (including in the DS), such as imbalances in excitatory and inhibitory neurotransmission, with ethanol consumption and preference (Bocarsly et al., 2019; Chen et al., 2011; Patton et al., 2021; Salinas et al., 2021). Our findings further support a role for the DS and suggest that imbalances in TLR3 and GABAergic signaling also regulate ethanol drinking. There is also evidence that ethanol consumption produces imbalances between TLR4 and TLR3 pathways that could drive drinking (McCarthy et al., 2018; Muralidharan et al., 2018; Warden et al., 2019a).

We accomplished our initial goal to develop a mouse model to determine if TLR3 signaling within the brain regulates ethanol consumption. In examining a potential mechanism for TLR3 modulation of ethanol drinking after DS-specific knockdown, we focused on those phenotypes that differed in global *Tlr3* knockout mice (Blednov et al., 2021). Thus, we tested recovery from ethanol-induced ataxia and AFT to ethanol since global knockout mice did not differ in any other behaviors that correlate with ethanol intake (e.g., severity of ethanol withdrawal, conditioned place preference, or conditioned taste aversion). Because the striatum is critical for controlling movement, however, testing a different ethanol behavior that does not depend on motor function is warranted in future studies. There were no changes in ethanol drinking after *Tlr3* knockout in the NAc or mPFC, so we did not pursue further testing in these mice. Given that the circuitry mediating voluntary ethanol consumption may be different than that for AFT, it will be important to determine if knockdown in the other regions could also alter AFT to ethanol. Future goals will be to explore cell type-specific and potential intracellular and circuit mechanisms underlying the ethanol-related behaviors, such as altered GABAergic or neuroimmune signaling.

5. Conclusions

We produced a conditional *Tlr3* knockout mouse model that provides the first evidence that brain-region specific TLR3 signaling can alter acute behavioral responses to ethanol that impact voluntary drinking. Compared with global knockout or systemic activation, these findings indicate a more direct role for TLR3 in the brain. We propose that inhibition of TRIF-dependent signaling in the DS is a potential strategy to reduce excessive ethanol consumption. Although TLR3 is an innate immune receptor, we do not know if it drives ethanol consumption by increasing neuroimmune responses or by other mechanisms, such as altered GABAergic signaling. *Tlr3* knockdown occurred predominantly in DS neurons, suggesting a neuronal mechanism in regulation of ethanol drinking. Further investigation of *Tlr3* knockdown in specific cell types will be necessary to determine if neuronal knockdown alone is sufficient to reduce alcohol consumption. Our *Tlr3*$^{F/F}$ mouse model provides a new tool to study brain regional and cell-type specificity of ethanol and immune responses.

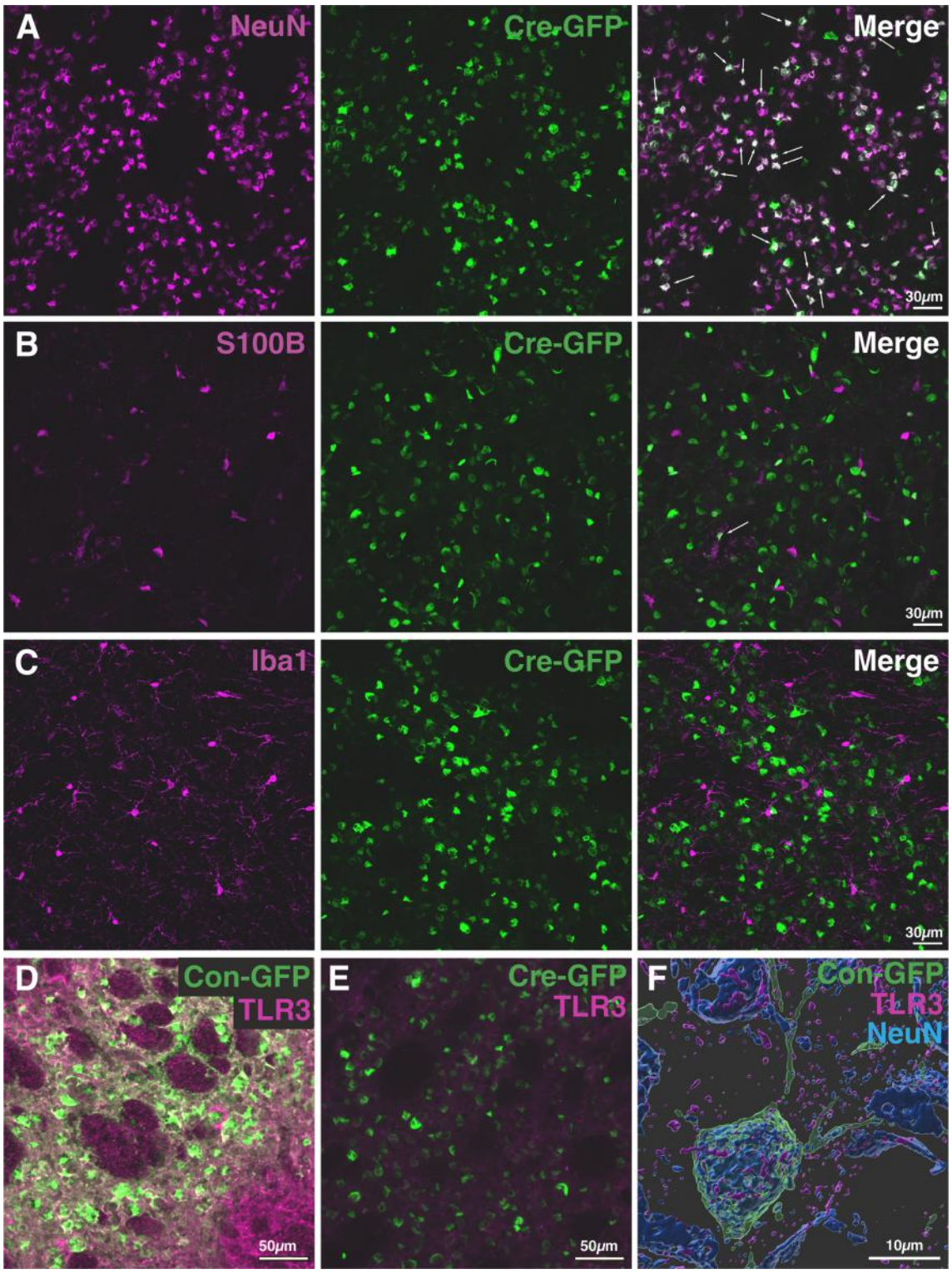

Fig. 7. TLR3 colocalization with cell-type markers in the dorsal striatum. (A-C) Immunofluorescence detection of GFP and **(A)** NeuN (neuronal nuclei, RBFOX3) for neurons, (**B**) S100B (S100 calcium-binding protein B) for astrocytes, and (**C**) Iba1 (Ionized calcium binding adaptor molecule 1) for microglia in mouse dorsal striatum 4 weeks after injection of AAV5-CMV-Cre-GFP. Representative examples of neurons (**A**) or astrocytes (**B**) that are colocalized with GFP are marked with white arrows in the merged images. **(D, E)** Sections of dorsal striatum from mice injected with AAV5-CMV-Control-GFP (**D**) or AAV5-CMV-Cre-GFP (**E**) showing overlay of TLR3 and GFP immunoreactivity. (**F**) 3-D reconstruction of section from a mouse injected with AAV5-CMV-Control-GFP showing colocalization of TLR3, GFP, and NeuN immunoreactivity in a striatal neuron.

CRediT authorship contribution statement

Geoffrey A. Dilly: Conceptualization, Formal analysis, Investigation, Writing – original draft, Writing – review & editing, Validation, Visualization. **Yuri A. Blednov:** Conceptualization, Formal analysis, Funding acquisition, Investigation, Project administration, Supervision, Validation, Writing – original draft, Writing – review & editing, Visualization. **Anna S. Warden:** Investigation, Conceptualization. **Lubov Ezerskiy:** Investigation, Validation. **Caleb Fleischer:** Investigation, Resources. **Jesse D. Plotkin:** Investigation, Validation. **Shruti Patil:** Investigation. **Elizabeth A. Osterndorff-Kahanek:** Formal analysis, Investigation, Validation, Writing – review & editing, Visualization, Methodology. **Jody Mayfield:** Writing – original draft, Writing – review & editing, Visualization. **R. Dayne Mayfield:** Conceptualization, Funding acquisition, Project administration, Writing – review & editing, Validation. **Gregg E. Homanics:** Conceptualization, Funding acquisition, Methodology, Project administration, Resources, Writing – review & editing, Supervision, Validation, Writing – original draft, Visualization. **Robert O. Messing:** Conceptualization, Formal analysis, Funding acquisition, Methodology, Project administration, Supervision, Writing – original draft, Writing – review & editing, Visualization, Investigation, Validation.

Declaration of competing interest

The authors declare that they have no known competing financial interests or personal relationships that could have appeared to influence the work reported in this paper.

Data availability

Data will be made available on request.

Acknowledgements

Funding: This work was supported by the National Institutes of Health grants U01 AA013520 (YAB and ROM), U24 AA025479 (ROM), R01 AA012404 and U01 AA020926 (RDM), U01 AA020889 (GEH), and F31 AA029635 (GAD). The authors thank Carolyn Ferguson and Jessika Hutchinson for expert technical assistance.

Appendix A. Supplementary data

Supplementary data to this article can be found online at https://doi.org/10.1016/j.bbi.2024.03.021.

References

Bassett, A.R., Tibbit, C., Ponting, C.P., Liu, J.L., 2013. Highly efficient targeted mutagenesis of drosophila with the CRISPR/Cas9 system. Cell Rep. 4, 220–228. https://doi.org/10.1016/j.celrep.2013.06.020.

Biswas, N., Liu, S., Ronni, T., Aussenberg, S.E., Liu, W., Fujita, T., Wang, T., 2011. The ubiquitin-like protein PLIC-1 or ubiquilin 1 inhibits TLR3-trif signaling. PLoS One 6, e21153.

Blednov, Y.A., Black, M., Chernis, J., Da Costa, A., Mayfield, J., Harris, R.A., 2017. Ethanol consumption in mice lacking CD14, TLR2, TLR4, or MyD88. Alcohol. Clin. Exp. Res. 41, 516–530. https://doi.org/10.1111/acer.13316.

Blednov, Y.A., Da Costa, A., Mayfield, J., Harris, R.A., Messing, R.O., 2021. Deletion of Tlr3 reduces acute tolerance to alcohol and alcohol consumption in the intermittent access procedure in male mice. Addict. Biol. 26, e12932 https://doi.org/10.1111/adb.12932.

Blednov, Y.A., Da Costa, A., Mason, S., Mayfield, J., Moss, S.J., Messing, R.O., 2022. Apremilast-induced increases in acute ethanol intoxication and decreases in ethanol drinking in mice involve PKA phosphorylation of GABAA beta3 subunits. Neuropharmacology 220, 109255. https://doi.org/10.1016/j.neuropharm.2022.109255.

Bocarsly, M.E., da Silva, E.S.D., Kolb, V., Luderman, K.D., Shashikiran, S., Rubinstein, M., Sibley, D.R., Dobbs, L.K., Alvarez, V.A., 2019. A mechanism linking two known vulnerability factors for alcohol abuse: heightened alcohol stimulation and low striatal dopamine D2 receptors. Cell Rep. 29, e1145 https://doi.org/10.1016/j.celrep.2019.09.059.

Chen, G., Cuzon Carlson, V.C., Wang, J., Beck, A., Heinz, A., Ron, D., Lovinger, D.M., Buck, K.J., 2011. Striatal involvement in human alcoholism and alcohol consumption, and withdrawal in animal models. Alcohol. Clin. Exp. Res. 35, 1739–1748. https://doi.org/10.1111/j.1530-0277.2011.01520.x.

Cheng, Y., Huang, C.C.Y., Ma, T., Wei, X., Wang, X., Lu, J., Wang, J., 2017. Distinct synaptic strengthening of the striatal direct and indirect pathways drives alcohol consumption. Biol. Psychiatry 81, 918–929. https://doi.org/10.1016/j.biopsych.2016.05.016.

Clarke, R., Adermark, L., 2015. Dopaminergic regulation of striatal interneurons in Reward and addiction: focus on alcohol. Neural Plast. 2015, 814567 https://doi.org/10.1155/2015/814567.

Cong, L., Ran, F.A., Cox, D., Lin, S., Barretto, R., Habib, N., Hsu, P.D., Wu, X., Jiang, W., Marraffini, L.A., Zhang, F., 2013. Multiplex genome engineering using CRISPR/Cas systems. Science 339, 819–823. https://doi.org/10.1126/science.1231143.

Crews, F.T., Qin, L., Sheedy, D., Vetreno, R.P., Zou, J., 2013. High mobility group box 1/Toll-like receptor danger signaling increases brain neuroimmune activation in alcohol dependence. Biol. Psychiatry 73, 602–612. https://doi.org/10.1016/j.biopsych.2012.09.030.

Cunningham, C., Campion, S., Teeling, J., Felton, L., Perry, V.H., 2007. The sickness behaviour and CNS inflammatory mediator profile induced by systemic challenge of mice with synthetic double-stranded RNA (poly I:C). Brain Behav. Immun. 21, 490–502. https://doi.org/10.1016/j.bbi.2006.12.007.

Erickson, E.K., Grantham, E.K., Warden, A.S., Harris, R.A., 2019. Neuroimmune signaling in alcohol use disorder. Pharmacol. Biochem. Behav 177, 34–60. https://doi.org/10.1016/j.pbb.2018.12.007.

Erwin, V.G., Deitrich, R.A., 1996. Genetic selection and characterization of mouse lines for acute functional tolerance to ethanol. J. Pharmacol. Exp. Ther. 279, 1310–1317.

Gano, A., Lebonville, C.L., Becker, H.C., 2022. TLR3 activation with poly I: C exacerbates escalated alcohol consumption in dependent male C57BL/6J mice. Am. J. Drug Alcohol Abuse 1–12. https://doi.org/10.1080/00952990.2022.2092492.

Hsu, P.D., Scott, D.A., Weinstein, J.A., et al., 2013. DNA targeting specificity of RNA-guided Cas9 nucleases. Nat. Biotechnol. 31, 827–832. https://doi.org/10.1038/nbt.2647.

Kawasaki, T., Kawai, T., 2014. Toll-like Receptor Signaling Pathways. Front Immunol. 5, 461. https://doi.org/10.3389/fimmu.2014.00461.

Lester, S.N., Li, K., 2014. Toll-like receptors in antiviral innate immunity. J. Mol. Biol. 426, 1246–1264. https://doi.org/10.1016/j.jmb.2013.11.024.

Lindefors, N., 1993. Dopaminergic regulation of glutamic acid decarboxylase mRNA expression and GABA release in the striatum: a review. Prog. Neuropsychopharmacol. Biol. Psychiatry 17, 887–903. https://doi.org/10.1016/0278-5846(93)90018-n.

Livak, K.J., Schmittgen, T.D., 2001. Analysis of relative gene expression data using real-time quantitative PCR and the 2(-Delta Delta C(T)) method. Methods 25, 402–408. https://doi.org/10.1006/meth.2001.1262.

Lovelock, D.F., Randall, P.A., Van Voorhies, K., Vetreno, R.P., Crews, F.T., Besheer, J., 2022. Increased alcohol self-administration following repeated toll-like receptor 3 agonist treatment in male and female rats. Pharmacol. Biochem. Behav 216, 173379. https://doi.org/10.1016/j.pbb.2022.173379.

McCarthy, G.M., Warden, A.S., Bridges, C.R., Blednov, Y.A., Harris, R.A., 2018. Chronic ethanol consumption: role of TLR3/TRIF-dependent signaling. Addict. Biol. 23, 889–903. https://doi.org/10.1111/adb.12539.

Mele, M., Costa, R.O., Duarte, C.B., 2019. Alterations in GABA(A)-receptor trafficking and synaptic dysfunction in brain Disorders. Front. Cell. Neurosci. 13, 77. https://doi.org/10.3389/fncel.2019.00077.

Melendez, R.I., 2011. Intermittent (every-other-day) drinking induces rapid escalation of ethanol intake and preference in adolescent and adult C57BL/6J mice. Alcohol. Clin. Exp. Res. 35, 652–658. https://doi.org/10.1111/j.1530-0277.2010.01383.x.

Meredith, L.R., Burnette, E.M., Grodin, E.N., Irwin, M.R., Ray, L.A., 2021. Immune treatments for alcohol use disorder: a translational framework. Brain Behav. Immun. 97, 349–364. https://doi.org/10.1016/j.bbi.2021.07.023.

Muralidharan, S., Lim, A., Catalano, D., Mandrekar, P., 2018. Human binge alcohol intake inhibits TLR4-MyD88 and TLR4-TRIF responses but not the TLR3-TRIF pathway: HspA1A and PP1 play selective regulatory roles. J. Immunol. 200, 2291–2303. https://doi.org/10.4049/jimmunol.1600924.

Patton, M.S., Heckman, M., Kim, C., Mu, C., Mathur, B.N., 2021. Compulsive alcohol consumption is regulated by dorsal striatum fast-spiking interneurons. Neuropsychopharmacology 46, 351–359. https://doi.org/10.1038/s41386-020-0766-0.

Pfaffl, M.W., 2001. A new mathematical model for relative quantification in real-time RT-PCR. Nucleic Acids Res. 29, e45.

Qin, L., Crews, F.T., 2012. Chronic ethanol increases systemic TLR3 agonist-induced neuroinflammation and neurodegeneration. J. Neuroinflammation 9, 130. https://doi.org/10.1186/1742-2094-9-130.

Ramos, A., Joshi, R.S., Szabo, G., 2022. Innate immune activation: Parallels in alcohol use disorder and Alzheimer's disease. Front. Mol. Neurosci. 15, 910298 https://doi.org/10.3389/fnmol.2022.910298.

Randall, P.A., Vetreno, R.P., Makhijani, V.H., Crews, F.T., Besheer, J., 2019. The toll-like receptor 3 agonist Poly(I:C) induces rapid and lasting changes in gene expression related to glutamatergic function and increases ethanol self-Administration in Rats. Alcohol. Clin. Exp. Res. 43, 48–60. https://doi.org/10.1111/acer.13919.

Renaud, J.B., Boix, C., Charpentier, M., et al., 2016. Improved genome editing efficiency and flexibility using modified oligonucleotides with TALEN and CRISPR-Cas9 nucleases. Cell Rep.. 14, 2263–2272. https://doi.org/10.1016/j.celrep.2016.02.018.

Rosenwasser, A.M., Fixaris, M.C., Crabbe, J.C., Brooks, P.C., Ascheid, S., 2013. Escalation of intake under intermittent ethanol access in diverse mouse genotypes. Addict. Biol. 18, 496–507. https://doi.org/10.1111/j.1369-1600.2012.00481.x.

Saliba, R.S., Pangalos, M., Moss, S.J., 2008. The ubiquitin-like protein Plic-1 enhances the membrane insertion of GABAA receptors by increasing their stability within the endoplasmic reticulum. J. Biol. Chem. 283, 18538–18544. https://doi.org/10.1074/jbc.M802077200.

Salinas, A.G., Mateo, Y., Carlson, V.C.C., Stinnett, G.S., Luo, G., Seasholtz, A.F., Grant, K. A., Lovinger, D.M., 2021. Long-term alcohol consumption alters dorsal striatal dopamine release and regulation by D2 dopamine receptors in rhesus macaques. Neuropsychopharmacology 46, 1432–1441. https://doi.org/10.1038/s41386-020-00938-8.

Schindelin, J., Arganda-Carreras, I., Frise, E., et al., 2012. Fiji: an open-source platform for biological-image analysis. Nat. Methods 9, 676–682. https://doi.org/10.1038/nmeth.2019.

Truitt, JM, Blednov, YA, Benavidez, JM, et al., 2016. Inhibition of IKKbeta Reduces Ethanol Consumption in C57BL/6J Mice. eNeuro 3. 10.1523/ENEURO.0256-16.2016.

Vetreno, R.P., Qin, L., Coleman Jr., L.G., Crews, F.T., 2021. Increased toll-like receptor-MyD88-NFkappaB-proinflammatory neuroimmune signaling in the orbitofrontal cortex of humans with alcohol use disorder. Alcohol. Clin. Exp. Res. 45, 1747–1761. https://doi.org/10.1111/acer.14669.

Warden, A.S., Azzam, M., DaCosta, A., Mason, S., Blednov, Y.A., Messing, R.O., Mayfield, R.D., Harris, R.A., 2019a. Toll-like receptor 3 activation increases voluntary alcohol intake in C57BL/6J male mice. Brain Behav. Immun. 77, 55–65. https://doi.org/10.1016/j.bbi.2018.12.004.

Warden, A.S., Azzam, M., DaCosta, A., Mason, S., Blednov, Y.A., Messing, R.O., Mayfield, R.D., Harris, R.A., 2019b. Toll-like receptor 3 dynamics in female C57BL/6J mice: regulation of alcohol intake. Brain Behav. Immun. 77, 66–76. https://doi.org/10.1016/j.bbi.2018.12.006.

Yang, H., Wang, H., Jaenisch, R., 2014. Generating genetically modified mice using CRISPR/Cas-mediated genome engineering. Nat. Protoc. 9, 1956–1968. https://doi.org/10.1038/nprot.2014.134.